Different Routes in the Forward and Backward Occurrences of the Hydrogen Electrode Reaction on Pt Single Crystal Electrodes in Acid Solution

Hideaki KITA,* Yunzhi GAO, Shen YE, and Katsuaki SHIMAZU
Division of Material Science, Graduate School of Environmental Earth Science, Hokkaido University, Sapporo 060
(Received May 31, 1993)

The hydrogen evolution and ionization reactions were studied on Pt single crystal electrodes in N_2 or H_2 saturated, acidic solutions. The hydrogen evolution reaction was structure insensitive and the ionization reaction was structure dependent. The Tafel constants of the respective reactions, $\vec{\alpha}$ and $\overleftarrow{\alpha}$, and the reaction orders, $\vec{z}_{H^+}$ and $\overleftarrow{z}_{H^+}$, with respect to proton, did not satisfy the relationships, $\vec{\alpha}+\overleftarrow{\alpha}=2$ and $\overleftarrow{z}_{H^+}-\vec{z}_{H^+}=-2$, deduced by the rate-determining step which is the same for the hydrogen evolution and ionization reactions; The results were, $\vec{\alpha}+\overleftarrow{\alpha}\approx 4$ and $\overleftarrow{z}_{H^+}-\vec{z}_{H^+}\approx -4$. These suggest that the rate-determining steps is different for the evolution and ionization reactions in acidic solutions. A tentative model for the reaction routes was proposed.

The study of the hydrogen electrode reaction on platinum electrodes has a long history since the beginning of this century.[1—13] Though it is a prototype of the electrode reaction, some problems have been remaining unsolved. For example, the Tafel slope of −30 mV for the hydrogen evolution reaction in acidic solutions assumes the recombination mechanism at a small coverage of hydrogen. However, the platinum surface is fully covered with the adsorbed hydrogen at potentials of the hydrogen evolution. Now, new spectroscopic techniques for the surface survey have been developed extensively in the last decade. Particularly, the in-situ IR observation[12,13] gives essential information for adsorbate on the electrode surface. Recently, Nichols and Bewick[13] reported that the on-top H appears at potentials more negative than ca. 80 mV (RHE) on single and polycrystalline Pt electrodes in acidic solutions and concluded that the on-top H is responsible for the hydrogen evolution.

We have reexamined a general electrochemical behavior of the hydrogen evolution and ionization reactions on Pt single crystal electrodes. Special caution was paid to reduce the effect of H_2 diffusion in solution by rotating the single crystal electrode which keeps the contact with solution through meniscus. The observed kinetics of the hydrogen evolution and ionization in acidic solutions reveal interesting features which contradict the expectation from a simple reaction theory. The present results lead us to conclude that the rate-determining step combined with the rapid hydrogen ion discharge step differs in the forward (evolution) and backward (ionization) directions, even on the same crystal plane in acidic solution.

Theoretical Relationship between Kinetic Parameters

Before describing our experimental results, we first derive the theoretically expected relationships between the Tafel constants, α's, and the reaction orders, z's, of the hydrogen electrode reaction.

The Tafel Constants. If a surface reaction consists of a series of elementary steps, and the r-th step is rate-determining, the electrochemical free energy change of the whole reaction, ΔG, is equal to the electrochemical free energy change of the rate-determining step, ΔG_r, multiplied by ν_r, where ν_r is the stoichiometric number[14] of the rate-determining step. Namely, when the whole reaction occurs once, the rate-determining step occurs ν_r times. Thus we have,

$$\Delta G = \nu_r \cdot \Delta G_r. \tag{1}$$

By the relation of $\Delta G = nF\eta$, we have,

$$\Delta G_r = \frac{nF\eta}{\nu_r}. \tag{2}$$

Where n is the numbers of the electrons concerned in the reaction. The general reaction rate expression of the forward and backward elementary steps is given as follows,[14]

$$\vec{v} = \frac{kT}{h} \cdot \exp\left(-\frac{\mu - \mu_I}{RT}\right), \tag{3}$$

and

$$\overleftarrow{v} = \frac{kT}{h} \cdot \exp\left(-\frac{\mu - \mu_F}{RT}\right), \tag{4}$$

where $\vec{v}$ and $\overleftarrow{v}$ are reaction rates of the forward and backward reactions, μ, μ_I, and μ_F are the electrochemical potentials of activated complex, initial system (reactant) and final system (product), respectively. Then, the difference between $\overleftarrow{v}$ and $\vec{v}$ gives the net rate and is expressed in terms of current for the hydrogen electrode reaction ($n=2$) as

$$\begin{aligned} j &= \overleftarrow{j}_r - \vec{j}_r = 2e(\overleftarrow{v} - \vec{v}) = \overleftarrow{j}_r \left(1 - \frac{\vec{j}_r}{\overleftarrow{j}_r}\right) \\ &= \overleftarrow{j}_r \{1 - \exp(-\Delta G_r / RT)\} \end{aligned} \tag{5}$$

where j, $\overleftarrow{j}_r$ and $\vec{j}_r$ are current densities of net, forward and backward reactions, and $\Delta G_r = \mu_F - \mu_I$. Introducing Eq. 2 into Eq. 5, and expanding the exponential term

at the conditions of $|\eta| \ll RT/F$ and $\overleftarrow{j}_r \simeq j_o$ (j_o is the exchange current density), one obtains

$$j = j_o \cdot \frac{nf\eta}{\nu_r}. \tag{6}$$

where $f = F/RT$.

On the other hand, j is related to the Tafel constants by the Butler–Volmer equation:

$$j = j_o \{\exp(\overleftarrow{\alpha} f\eta) - \exp(-\vec{\alpha} f\eta)\}. \tag{7}$$

where $\vec{\alpha}$ and $\overleftarrow{\alpha}$ are the Tafel constants for the hydrogen evolution and ionization reactions, respectively. As $|\eta| \ll RT/F$, expansion of the exponential term leads:

$$j = j_o (\overleftarrow{\alpha} + \vec{\alpha}) f\eta. \tag{8}$$

Comparison of Eqs. 6 and 8 yields

$$\overleftarrow{\alpha} + \vec{\alpha} = \frac{n}{\nu_r}. \tag{9}$$

Reaction Orders. Nernst's equation is generally expressed as

$$\phi_{eq} = \phi_0 + \frac{1}{nf} \times \ln \prod_k (a_k{}^{m_k}), \tag{10}$$

where ϕ_{eq} and ϕ_0 are equilibrium and standard potential, a_k and m_k are activity and the coefficient of k species in an electrode reaction. When k is reactant, m_k has a negative value, and when k is product, m_k has a positive value, respectively. A similar equation is derived from kinetic expressions of j_o which are given in general form for forward and backward reactions as

$$j_o = \vec{k} \cdot \exp(-\vec{\alpha} f\phi_{eq}) \cdot \prod_k \left(a_k{}^{\vec{z}_k}\right), \tag{11}$$

and

$$j_o = \overleftarrow{k} \cdot \exp(-\overleftarrow{\alpha} f\phi_{eq}) \cdot \prod_k \left(a_k{}^{\overleftarrow{z}_k}\right), \tag{12}$$

where $\vec{k}$ and $\overleftarrow{k}$ are rate constants and $\vec{z}_k$ and $\overleftarrow{z}_k$ are the reaction orders with respect to the species k in the hydrogen evolution and ionization reactions. By equating Eqs. 11 and 12, we have

$$\phi_{eq} = \frac{1}{(\overleftarrow{\alpha} + \vec{\alpha}) f} \cdot \ln \frac{\overleftarrow{k}}{\vec{k}} + \frac{1}{(\overleftarrow{\alpha} + \vec{\alpha}) f} \cdot \ln \prod_k a_k{}^{(\overleftarrow{z}_{H^+} - \vec{z}_{H^+})}, \tag{13}$$

Introduction of Eq. 9 into Eq. 13 gives

$$\phi_{eq} = \frac{1}{nf} \cdot \ln \frac{\overleftarrow{k}}{\vec{k}} + \frac{1}{nf} \cdot \ln \prod_k a_k{}^{(\overleftarrow{z}_{H^+} - \vec{z}_{H^+})\nu_r}. \tag{14}$$

Comparison of the last terms of Eqs. 10 and 14 yields

$$\overleftarrow{z}_k - \vec{z}_k = \frac{m_k}{\nu_r}. \tag{15}$$

The hydrogen electrode reaction at Pt in acidic solutions is generally accepted as consisting of two elementary steps; the discharge step and the recombination step, where the latter step,

$$H(a) + H(a) \rightarrow H_2$$

is rate-determining. Then we have, $\nu_r = 1$, $m_H = -2$, and $n = 2$. Thus Eqs. 9 and 15 become

$$\overleftarrow{\alpha} + \vec{\alpha} = 2 \tag{16}$$

$$\overleftarrow{Z}_{H^+} - \vec{Z}_{H^+} = -2 \tag{17}$$

Experimental

Platinum single crystals were prepared using Clavilier's method.[15,16] In this experiment, three low index planes of (111), (100), and (110) were used. Before each measurements, the electrode was annealed in a gas+oxygen flame at 600 °C for a few seconds and then quenched with Milli-Q water and mounted onto cell.

At measurements, the crystal was rotated, keeping the plane of interest in contact with the solution through meniscus. Recently, the same method has been used by Cahan and Villullas[17] in studies of the ferri-ferro redox system at a gold single crystal disc electrode. The rotation speed was varied in the range 500—5000 rev·min^{-1} (Nikko Keisoku, RRDE-1).

Electrolytic solutions of sulfuric acid solution with Na_2SO_4 to keep the ionic strength at 0.5 M were prepared from suprapure reagents (Wako Pure Chemical CO.) and Milli-Q water (Millipore Corp., MA). Cyclic voltammograms (CV) and stationary currents were recorded by an usual instrument (POTENTIOSTAT/GALVANOSTAT 2001 and FUNCTION GENERATOR FG-02, TOHO Technical Research, Japan). All measurements were conducted at room temperature. Potentials in the text were referred to the reversible hydrogen electrode (RHE) in the same solution.

Results and Discussion

Before every measurement, CV with a sweep rate of 50 mV s^{-1} was taken and used as a criterion for the identification and cleanliness of the respective planes of Pt single crystal electrodes.

Adsorbed Hydrogen on the Respective Crystal Planes. We first present the hydrogen waves observed at Pt(111), (100), and (110) in 0.5 M H_2SO_4 in Fig. 1 (100 mV s^{-1}). Each voltammogram shows a symmetrical pattern with respect to the potential axis, demonstrating that the discharge step is rapid enough to be assumed in equilibrium,

$$H^+ + e^- \rightleftharpoons H(a),$$

where (a) denotes the adsorbed state. The electricity estimated from the wave area indicates that the hydrogen atom adsorbs to a full coverage with a 1 to 1 correspondence with the surface Pt atom at 50 mV, though Pt(110) reveals an exceptionally high coverage of 1.4—1.5.

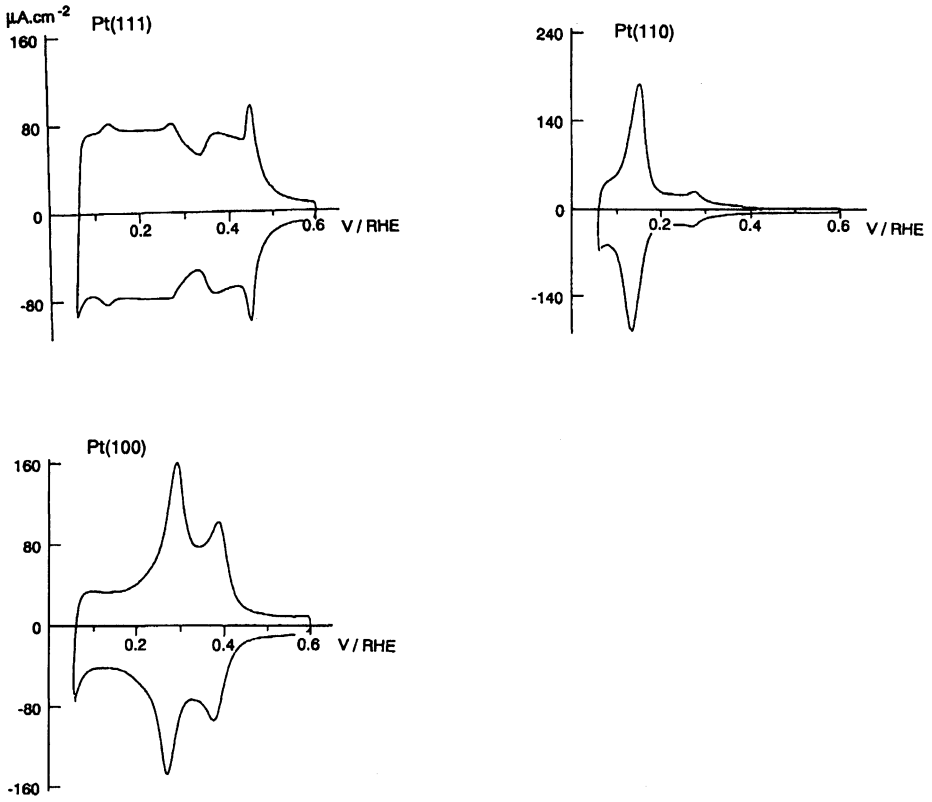

Fig. 1. Cyclic voltammograms of Pt(111), Pt(110), and Pt(100) electrodes in 0.5 M H_2SO_4. Sweep rate, 100 $mV\,s^{-1}$.

It is one of the interests in the present work whether the adsorbed hydrogen take part in the hydrogen evolution and ionization reactions or not. These hydrogens are denoted UPD-H in the text.

Kinetics for the Forward Hydrogen Electrode Reaction (Evolution). We have already reported the kinetic parameters on the respective electrodes in 0.5 M H_2SO_4.[18] The Tafel relation was not affected by the rotation speed from 500 to 5000 rev·min^{-1}. The kinetic parameters obtained at 1000 rev·min^{-1} are quoted in Table 1. The Tafel constant $\vec{\alpha}$ and $\log j_0$ (exchange current density) are common among the electrodes studied, indicating structure insensitiveness of the hydrogen evolution reaction. The structure insensitiveness will reflect that the real reaction intermediate for the forward hydrogen electrode reaction is common among the crystal planes, i.e., the on-top H as concluded by Nichols and Bewick[13] and not the structure sensitive UPD-H. A similar conclusion is reported recently by Lei et al.[19] by coulometric study.

Table 1. Kinetic Parameters of the Hydrogen Evolution and Ionization Reactions in Acid Solution

Plane	(111)	(100)	(110)
[H_2 evolution]			
$\log j_0/A\,cm^{-2}$	−2.99	−2.97	−2.87
Tafel slope/mV	−34	−35	−32
$\vec{\alpha}$	1.8	1.7	1.9
$\vec{Z}_{H^+}$	1.7	1.7	1.9
[H_2 ionization]			
Tafel slope/mV	45	45	35
$\overleftarrow{\alpha}$	1.3	1.3	1.7
$\overleftarrow{Z}_{H^+}$	−1.3	−1.3	−1.7
$\overleftarrow{\alpha}+\vec{\alpha}$	3.1	3.0	3.6
$\overleftarrow{Z}_{H^+}-\vec{Z}_{H^+}$	−3.0	−3.0	−3.6

When $\log \vec{j}$ is plotted against η, the plot appears independent of pH in a range from 0.1 to 2.5 on the respec-

In the present work, the reaction order with respect to H^+, $\vec{z}_H$, was examined. $\vec{z}_H$ is defined as

$$\vec{Z}_{H^+} \equiv \left(\frac{\partial \log \vec{j}}{\partial \log a_{H^+}}\right)_{\phi}, \tag{18}$$

where ϕ is the electrode potential referred to the standard hydrogen electrode and a_H is the activity of H^+, respectively. The above reaction order is expressed as[20]

$$\vec{Z}_{H^+} = \vec{Z}'_{H^+} - \frac{m_{H^+}}{n}\vec{\alpha} \tag{19}$$

in terms of the apparent reaction order defined at a constant overvoltage (η) as

$$\vec{Z}'_{H^+} \equiv \left(\frac{\partial \log \vec{j}}{\partial \log a_{H^+}}\right)_{\eta} \tag{20}$$

and the numbers of H^+ and electron concerned in the reaction, m_H and n. The value of m has negative sign for the reaction.

tive planes within an experimental error, i.e., $Z'_{H^+}=0$ (Fig. 2). The values of Z_{H^+} from Eq. 19 with $m_{H^+}=-2$ and $n=2$ are 1.7—1.9, close to 2 and listed in Table 1.

Kinetics for the Backward Reaction of the Hydrogen Electrode Reaction. When hydrogen was introduced into the electrolyte solution, the reversible hydrogen electrode holds and a positive polarization causes the hydrogen ionization reaction. Figure 3 represents a typical polarization curve at Pt(110) in H_2-saturated 0.5 M H_2SO_4 (sweep rate 5 mV s^{-1}, 1000 rev·min^{-1}). The anodic current rapidly increases with the polarization and at ca. 70 mV reaches a limiting value, j_L, which depends on the rotation speed of the electrode. j_L observed at 115 mV by sweeping the rotation speed up and down (20 rev·min^{-1}) is plotted against $\omega^{1/2}$ in Fig. 4. The Levich relation holds,

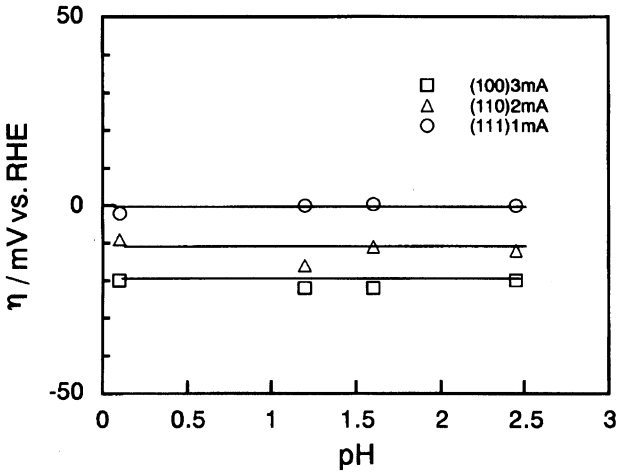

Fig. 2. pH effect of the overvoltage at 1 mA cm^{-2} on Pt(111), 2 mA cm^{-2} on Pt(110) and 3 mA cm^{-2} on Pt(100). Solution, $H_2SO_4+Na_2SO_4$ (ionic strength, 0.5 M).

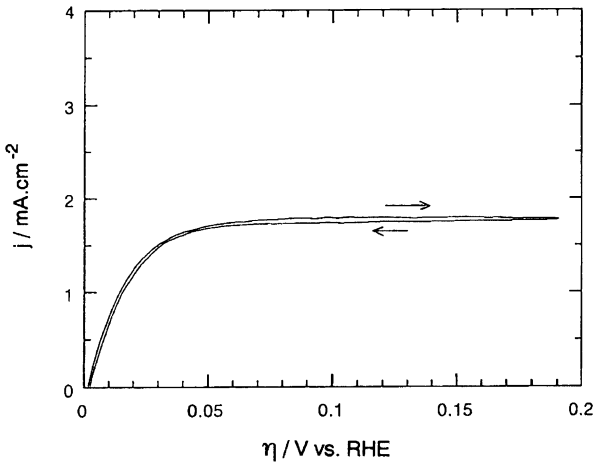

Fig. 3. Positive and negative polarization curves for H_2 ionization at the rotating Pt(110) electrode in H_2 saturated 0.5 M H_2SO_4. Sweep rate, 5 mV s^{-1}. Rotation speed, 1000 rev·min^{-1}.

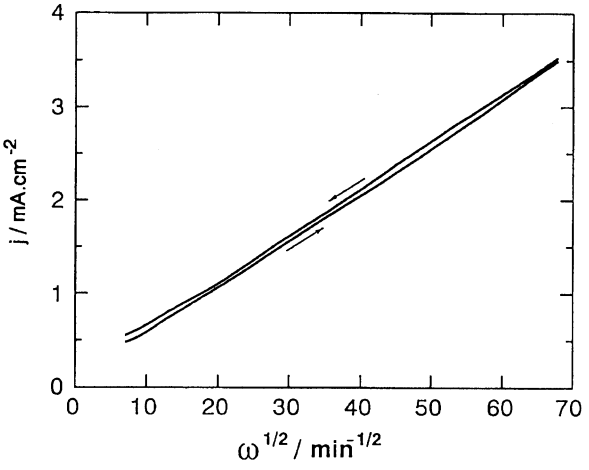

Fig. 4. The Levich plot for H_2 ionization on the rotating Pt(110) electrode in H_2 saturated 0.5 M H_2SO_4. Rotation sweep speed, 20 rev·min^{-1} s^{-1}. Electrode potential, 115 mV vs. RHE.

demonstrating that j_L is controlled by the H_2 diffusion (denoted j_{DL} in what follows). At a smaller polarization, the hydrogen ionization is mix-controlled by the H_2 diffusion (in solution) and the backward reaction (at surface). In order to obtain the kinetic parameters of the surface backward reaction, we treated the polarization curve as follows.

By using the surface concentration of H_2, the net current j is expressed by:

$$j = \overleftarrow{j} - \overrightarrow{j} = j_o\left\{\exp\left(\overleftarrow{\alpha} f\eta\right)\cdot\left(\frac{C_{H_2,s}}{C_{H_2,b}}\right) - \exp\left(-\overrightarrow{\alpha} f\eta\right)\right\}, \tag{21}$$

where $\overleftarrow{j}$ and $\overrightarrow{j}$ are the backward and forward current densities of the surface reaction, $C_{H_2,s}$ and $C_{H_2,b}$ the concentrations of hydrogen near the surface and in the bulk, and $f \equiv F/RT$, respectively. From Fick's second law, the concentration ratio in the above equation is expressed as

$$\frac{C_{H_2,s}}{C_{H_2,b}} = 1 - \frac{j}{j_{DL}}, \tag{22}$$

where j_{DL} is given in terms of the diffusion coefficient, D, and the diffusion layer thickness, δ, as $j_{DL} = nFDC_{H_2,b}/\delta$. Introduction of Eq. 21 to Eq. 22, yields

$$j = j_o\left\{\exp\left(\overleftarrow{\alpha} f\eta\right)\cdot\left(1 - \frac{j}{j_{DL}}\right) - \exp\left(-\overrightarrow{\alpha} f\eta\right)\right\}. \tag{23}$$

Since j_o, j, and $\overrightarrow{\alpha}$ in Eq. 23 were already given from the hydrogen evolution experiments, the Tafel constant $\overleftarrow{\alpha}$ of the backward reaction can be obtained by plotting $\log \overleftarrow{j}$ against η, where $\log \overleftarrow{j}$ is given from Eq. 23 as

$$\log\left[\frac{j/j_o + \exp\left(-\frac{\overrightarrow{\alpha} F}{RT}\eta\right)}{1 - j/j_{DL}}\right]$$

Figure 5 exemplifies the results at the respective planes in the H_2-saturated 0.1 M H_2SO_4 for 1000 rev·min^{-1}. The slopes give the Tafel constants summarized in Table 1. We find that $\overleftarrow{\alpha}$ is almost the same at (111) and (100), 1.3, and clearly larger at Pt(110), 1.7. These values, independent of ω in a range of 500—5000 rev·min^{-1}, indicates that the hydrogen ionization reaction is structure sensitive.

Once the $\overleftarrow{\alpha}$ becomes known, $\overleftarrow{j}$ and hence the Tafel line for the backward reaction under the absence of the diffusion control is calculated. Thus, the reaction order of hydrogen ion for the backward reaction,

$$\overleftarrow{Z}_{H^+} \equiv \left(\frac{\partial \log \overleftarrow{j}}{\partial \log a_{H^+}}\right)_{\phi} \tag{24}$$

can be estimated from the results obtained at various pH (0.1—1.7). A similar relation to Eq. 19,

$$\overleftarrow{Z}_{H^+} = \overleftarrow{Z}'_{H^+} - \frac{m_{H^+}}{n}\overleftarrow{\alpha}$$

was used where $\overleftarrow{Z}'_{H^+}$ is the reaction order defined at a constant overvoltage. Reaction orders thus obtained on Pt(111), (100), and (110) are shown in Table 1.

Discussion on the Reaction Route of the Hydrogen Electrode Reaction. The obtained kinetic parameters disagree with the theoretically expected values described in the previous section. The experimental values in Table 1 give $\overleftarrow{\alpha}+\overrightarrow{\alpha}=3.0$—3.6 and $\overleftarrow{z}_{H^+}-\overrightarrow{z}_{H^+}=-3.0$——3.6 in acidic solutions, being entirely different from the theoretically expected values ($\overleftarrow{\alpha}+\overrightarrow{\alpha}=2$ and $\overleftarrow{z}_{H^+}-\overrightarrow{z}_{H^+}=-2$). The discrepancy in acidic solutions undoubtedly denies our tacit assumption that the rate-determining step occurs in the forward and backward directions via the same potential profile. In other words, the above discrepancy leads us to assume different routes for the rate-determining step in the forward (evolution) and backward (ionization) direction at Pt in acidic solutions.

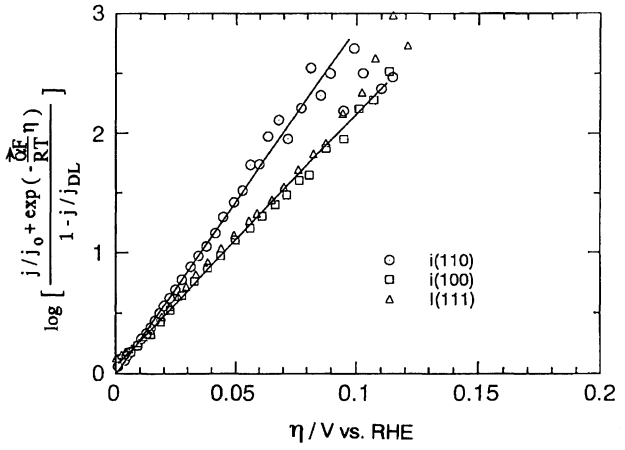

Fig. 5. Tafel polts of H_2 ionization reaction on rotating Pt(111), Pt(110), and Pt(100) in 0.1 M H_2SO_4+ 0.9 M Na_2SO_4. Rotation speed, 1000 rev·min^{-1}.

One of the possible explanations is illustrated in Fig. 6a. The forward reaction may take place on terrace of the Pt crystal planes at which the sites of the rate-determining step must be different from the ones for the UPD-H familiar from the voltammogram, since the hydrogen evolution reaction rate appears structure insensitive. On the other hand, in the case of the backward reaction, hydrogen molecule first adsorbs on the defects such as steps or kinks, as shown in Fig. 6a which will have a higher adsorption energy than the terrace. In fact, in gas/solid system it is reported that hydrogen molecule undergoes easily dissociative adsorption at steps on the single crystal of platinum.[21] These dissociated hydrogen atoms may either move to terrace by surface diffusion, or ionize directly to H^+. Easier recombinative desorption on terrace and easier dissociative adsorption at steps will be reasonably accepted, provided that the heat of adsorption is larger at defects than at terrace.

The other explanation is illustrated in Fig. 6b. The forward reaction will take place at the on-top H site and the backward reaction at the UPD-H site, respectively.

The hydrogen evolution proceeds by the recombination of the on-top H where the UPD-H of full cover-

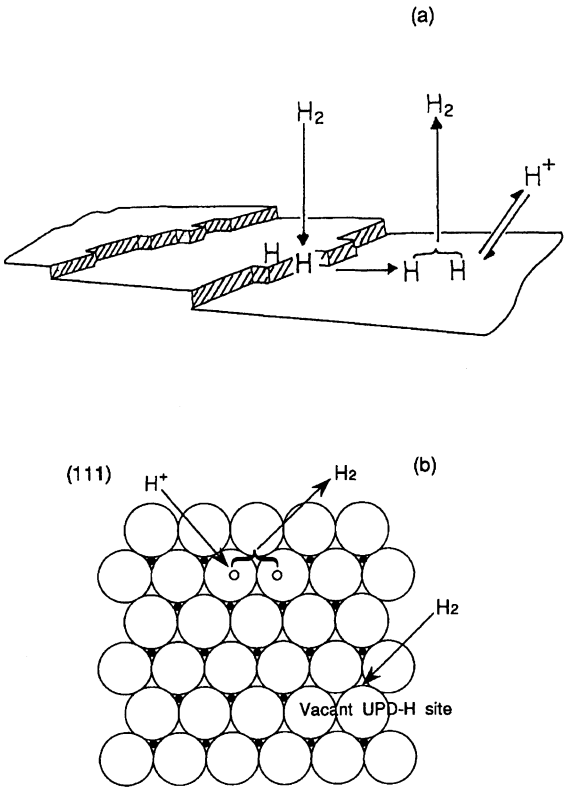

Fig. 6. (a) A possible model for the hydrogen evolution and ionization at Pt electrode. (b) Another model for the hydrogen evolution reaction (at on-top H site) and hydrogen ionization reaction (at UPD-H site). A pair of on-top H's (O), each occupying the sites of the adjacent platinum atoms, undergoes the recombination.

age does not take part in the reaction. Though the detailed way of the recombination will remain open to discussion, Fig. 6b shows one of the possible ways that a pair of on-top H's, each occupying the on-top site of the adjacent platinum atoms, undergoes the recombination. The on-top H population will increase proportional to $\exp(-\eta F/RT)$ at a low coverage which leads to the Tafel slope of -30 mV. Energetics of the on-top H will be primarily determined by the nature of the surface atom itself and only secondarily by the surface arrangements. This is in agreement with the structure insensitiveness of the forward reaction.

The hydrogen ionization reaction is also controlled by the first elementary step of H_2 dissociation to the adsorbed hydrogen. This backward reaction will take place at a vacant UPD-H site which will be allowed to exist in a sensitive manner to the electrode potential in a coverage range of UPD-H close to unity. The energetics of the UPD-H site will be now affected by the surface arrangement of platinum atoms. The present results demonstrates the structure dependence of the backward reaction, showing a higher value of the Tafel slope at Pt(111) and (100) than that at Pt(110). The population of the vacant UPD-H site will be taken to increase proportionally to $\exp(-\eta F/RT)$ in a region close to the full coverage of UPD-H. The requirement of the adjacent pair of the vacant sites will bring the Tafel slope of 30 mV, while the electrochemical dissociative adsorption,

$$H_2 \rightarrow H(a) + H^+ + e^-$$

brings the Tafel slope of 40 mV.

Here we estimated the number of the reaction site (inperfections or vacant sites) which is effective under the mixed control of the surface reaction and the H_2 diffusion. First we assume a hexagonal distribution of the reaction site. Each reaction site forms its own semi-spherical diffusion layer during the reaction. The layer will grow with the reaction time and reach the maximum one at a radius, l, determined by the solution convection. The number of the semi-spheres which array in a hexagonal pattern is given at a radius of l as

$$N = \frac{1}{2\sqrt{3}} \cdot \frac{1}{l^2}$$

When l is 10^{-3} cm, N becomes 3×10^5 cm^{-2}. This number is extremely small compared to the atom numbers present in the surface, ca. 10^{15} cm^{-2}. N increases to 3×10^{11} cm^{-2} at $l=10^{-5}$ cm but still is less than 0.05% of the total atoms.

This means that the hydrogen ionization reaction reaches the limiting rate at an expense of the negligibly small amount of UPD-H.

For further detailed information, it is required to carry out the experiment at much more precisely controlled experimental conditions including the surface state.

References

1) J. Tafel, *Z. Phys. Chem.*, **50**, 641 (1905).
2) J. O'M. Bockris, *Chem. Rev.*, **43**, 525 (1948).
3) S. Schuldiner, *J. Electrochem. Soc.*, **99**, 488 (1952); **101**, 426 (1954); **106**, 89 (1956).
4) S. Schuldiner and J. P. Hoare, *Can. J. Chem.*, **37**, 228 (1959).
5) F. G. Will and C. A. Knorr, *Z. Electrochem.*, **64**, 258 (1960).
6) M. Breiter, "Transaction of the Symposium on the Electrode Processes," ed by E. Yeager, John Wiley & Sons, New York (1961), p. 307.
7) S. Schuldiner, M. Rosen, and D. Flinn, *J. Electrochem. Soc.*, **117**, 1251 (1970).
8) H. Kita, "Encyclopedia of Electrochemistry of the Elements," ed by A. J. Bard, Marcel Dekker, New York (1982), Vol. IX-A, p. 413.
9) M. Enyo, "Comprehensive Treatise of Electrochemistry," ed by E. Conway, Plenum, London (1983), Vol. 7, p. 241.
10) E. Conway and LiJun Bai, *J. Electroanal. Chem.*, **198**, 149 (1986).
11) K. Seto, A. Iannelli, BeLove, and Lipkowski, *J. Electroanal. Chem.*, **226**, 351 (1987).
12) J. Nichols and A. Bewick, *J. Electroanal. Chem.*, **107**, 205 (1980).
13) J. Nichols and A. Bewick, *J. Electroanal. Chem.*, **243**, 445 (1988).
14) J. Horiuti, *J. Res. Inst. Catalysis, Hokkaido Univ.*, **1**, 8 (1948).
15) J. Clavilier, R. Faure, G. Gunet, and R. Durand, *J. Electroanal. Chem.*, **107**, 205 (1980).
16) H. Kita, S. Ye, A. Aramata, and N. Furuya, *J. Electroanal. Chem.*, **295**, 245 (1990).
17) B. D. Caham and H. M. Villullus, *J. Electroanal. Chem.*, **307**, 263 (1991).
18) H. Kita, S. Ye, and Y. Gao, *J. Electroanal. Chem.*, **334**, 351 (1992).
19) H. Lei, B. Wu, and C. Cha, *J. Electroanal. Chem.*, **332**, 257 (1992).
20) H. Kita and K. Uosaki, "Denki Kagaku Kiso," Gihodo, Tokyo (1983), p. 161.
21) M. Salmeron, R. J. Gale, and G. A. Somorjai, *J. Chem. Phys.*, **67**, 5324 (1977).